Bull. Mater. Sci., Vol. 40, No. 6, October 2017, pp. 1203–1211
DOI 10.1007/s12034-017-1468-z

One-pot synthesis of CaAl-layered double hydroxide–methotrexate nanohybrid for anticancer application

MANJUSHA CHAKRABORTY[1], MANOJ K MITRA[2] and JUI CHAKRABORTY[1,*]

[1]Bioceramic and Coating Division, CSIR-Central Glass and Ceramic Research Institute, Kolkata 700 032, India

[2]Department of Metallurgical and Materials Engineering, Jadavpur University, Kolkata 700032, India

*Author for correspondence (jui@cgcri.res.in)

MS received 22 April 2016; accepted 12 February 2017; published online 26 September 2017

Abstract. One-pot (co-precipitation) synthesis route was employed for the first time to synthesize pristine CaAl-layered double hydroxide (LDH) and *in-situ* intercalation of the anticancer drug methotrexate (MTX) to prepare CaAl-LDH–MTX nanohybrid. An increase in the interplanar spacing of the (003) plane from 8.6 Å in pristine CaAl-LDH bilayered structure to 18.26 Å in CaAl-LDH–MTX nanohybrid indicated successful intercalation of anionic MTX into the interlayer space of CaAl-LDH. This was supported by the transmission electron micrographs, which showed an increase in average interlayer spacing from 8.7 Å in pristine LDH to 18.31 Å in LDH–MTX nanohybrid. Particle size and morphology analysis of pristine CaAl-LDH and LDH–MTX nanohybrid using both dynamic light scattering (DLS) technique and transmission electron microscopy (TEM) indicated a decrease in average particle size in LDH–MTX nanohybrid as compared with that of pristine LDH. Thermogravimetric analyses (TGA) revealed an enhancement in decomposition temperature of MTX bound to CaAl-LDH nanohybrid to 380°C as compared with 290°C in pure MTX molecule, indicating enhanced thermal stability, which supports stable electrostatic interaction of MTX within the interlayer position of LDH. CHN (carbon hydrogen nitrogen) analysis revealed nearly 49 wt% of MTX loading into CaAl-LDH, which closely matched with the result obtained from TGA of the nanohybrid. Cumulative release of MTX from CaAl-LDH–MTX in phosphate buffer solution showed a non-linear dependence with incubation time. Release mechanism of MTX from LDH–MTX nanohybrid was governed by diffusion mechanism at physiological pH of 7.4. The *in vitro* cytotoxicity study of LDH–MTX nanohybrid using MG-63 human osteosarcoma cell line indicated enhanced inhibition of the cancer cell proliferation compared with the MTX drug alone.

Keywords. Layered double hydroxide; one-pot synthesis; anticancer drug methotrexate; intercalation; release kinetics; controlled release.

1. Introduction

Recently, there has been rapid expansion of the development of bioinorganic hybrid systems for safe drug delivery, using biocompatible matrices [1,2]. In this regard, layered double hydroxides (LDHs) are well established as excellent anion exchange materials and their extensive intercalation chemistry has widespread applications in areas including medicine due to their unique host–guest-type structure [3,4]. LDHs are a class of synthetic two-dimensional nanostructured layered clay mineral derived from the structure of mineral brucite, $Mg(OH)_2$ [5,6]. Analogous to brucite, the LDH metal cations M^{2+} and M^{3+} are surrounded by six hydroxyl groups that share the edges to form an infinite sheet [3,7]. It can be prepared by different laboratory techniques [8], of which co-precipitation synthetic route is usually preferred for the preparation of organic anion-containing LDHs, which are difficult to obtain in other ways [10]. In general, co-precipitation is based on the slow addition of a mixed solution of divalent and trivalent metal salts to an alkaline solution in a reactor, which leads to the co-precipitation of the two metal salts [11,12] carried out at constant pH, which yields LDHs with good crystallinity, smaller average particle sizes, higher average specific surface area and higher average pore diameters along with accurate control of the charge density (M^{2+}/M^{3+} ratio, where M^{2+} is Mg, Ca, Zn Fe, Cu, Mn, etc. ions, and M^{3+} is Al, Fe, Cr, Co, etc.) [10].

In the drug–LDH composite the metal ions should be biocompatible in nature that permits safe retention as well as the controlled delivery of the drugs [13,14]. The cationic layered framework of LDH leads to safe accommodation of many biologically important molecules [15]. Apart from being a controlled release drug delivery system, LDHs also render high drug loadings, enhanced drug stability, sustained drug release, reduced toxicity, improved cellular uptake and even improved efficacy of drugs, in comparison with many of the existing systems [16,17]. LDHs are promising materials as drug delivery systems in biomedical research to transport and release anti-inflammatory or anticancer drugs [18]. Generally, the diffusion and dissolution mechanisms are considered for the release of the drugs from the LDH solid matrix at neutral and acidic conditions, respectively [19,20].

Among a range of LDHs used as drug delivery matrices, MgAl-LDH is the most widely explored one, on account of its intrinsic biocompatibility and structural conformity, due to the small ionic radius of the Mg^{2+} ion [3]. Replacing/substituting the bivalent metal cation of the hexagonal lattice by Zn^{2+}, also, does not change the size factor in the 2D layers of the same. However, further substitution of this material by another biocompatible cation, e.g., Ca^{2+}, might lead to structural instability, followed by imparting of its influence on the interaction between the charged brucite layers and hence affecting the interlayer space. This can be attributed to the microstrain or nonuniform strain exerted on the LDH bilayer, on account of the substitution of the Ca^{2+} ion having a larger ionic radius (114 pm) in place of Mg^{2+} ion, having an ionic radius of 86 nm only [8].

In this work, we demonstrate a fast one-pot synthetic strategy involving simultaneous co-precipitation and *in-situ* intercalation of MTX drug into the interlayer space of nanosized CaAl-LDH, as a biocompatible host. MTX is found to be effective in the treatment of certain human cancers such as osteosarcoma, leukaemia, etc. The route by which MTX shows its activity is that it inhibits the action of dihydrofolate reductase (DHFR). DHFR catalyses the reduction of the dihydrofolate to the tetrahydrofolate in a folate cycle coupled with DNA synthesis and cell proliferation. Thus, the influx of MTX into the cytosol eventually results in the cell apoptosis [9].

The chance of carbonate incorporation/contamination into the interlayer space of the LDH is less due to the short duration of the process. Although Plank *et al* [21] intercalated organic polycarboxylate polymers into CaAl- LDH, to the best of our knowledge there is no report in the published literature on the potential application of CaAl-LDH in the field of medicine, as a drug delivery vehicle. The synthesized LDH–MTX nanohybrid was characterized using powder X-ray diffraction (XRD), transmission electron microscopy (TEM), field emission scanning electron microscopy (FESEM), thermal analyses (thermogravimetry–differential thermal analysis (TG–DTA), Fourier transform infrared spectroscopy (FTIR) and dynamic light scattering (DLS) techniques. The loading capacity of methotrexate (MTX) in CaAl-LDH nanopowder was estimated using carbon, hydrogen and nitrogen (CHN) analyses supported by thermal analyses. The release behaviour of MTX from nanohybrid material under simulated physiological condition (pH 7.4) was studied using high performance liquid chromatography (HPLC).

2. Materials and methods

2.1 *Materials*

Calcium nitrate hexahydrate [$Ca(NO_3)_2 \cdot 6H_2O$], aluminium nitrate nonahydrate [$Al(NO_3)_3 \cdot 9H_2O$], sodium hydroxide and ammonium hydroxide (25%) were purchased from Merck, India (analytical grade). MTX ($\geq$98% purity) was procured from Sigma-Aldrich, USA. All the aqueous solutions in this study were prepared with deionized (Millipore, specific resistivity 18 MΩ) and decarbonated (by purging XL grade nitrogen) water. All the chemicals used in this study were used as received without further purification.

2.2 *Methods*

2.2a *One-pot synthesis and in-situ MTX intercalation in CaAl-LDH*: In the co-precipitation method, precursor solution containing 20 mmol $Ca(NO_3)_2 \cdot 6H_2O$ (Sigma-Aldrich) and 10 mmol $Al(NO_3)_3 \cdot 9H_2O$ (Sigma-Aldrich) in 250 ml decarbonated water was taken in a three-necked flask. From one neck of the flask, addition of an 0.01 M aqueous soution of NaOH was carried out drop-wise to the mixed solution with continuous stirring under nitrogen blanket (XL grade purity, 99.999%) along with the addition of 50 ml of 0.043 M drug (MTX) solution in decarbonated water of pH 7.5 from the other neck simultaneously with constant stirring and under nitrogen atmosphere. The pH of the reaction mixture was finally raised to the desired (9.6) value by drop-wise addition of the NaOH solution, to obtain *in situ* precipitated CaAl-LDH–MTX nanohybrid.

The whole process was carried out with continuous stirring and the reaction mixture was agitated for further 48 h. The resultant suspension of LDH–MTX was centrifuged, washed thrice using decarbonated water and finally freeze dried at -82°C and 20 Pa pressure to get dry CaAl-LDH–MTX nanopowder.

2.2b Preparation of samples for HPLC analysis: *In vitro* drug release of MTX-intercalated CaAl-LDH was carried out using a type-II USP dissolution rate test apparatus (Electrolab TDT-146 08L, Mumbai, India). To describe the method in brief, exactly 47.16 mg (CaAl-LDH–MTX) of drug-loaded sample (equivalent to 25 mg of drug in nanohybrid) was placed in 900 ml of phosphate-buffered saline (PBS) solution of pH 7.4 while maintaining $37 \pm 2^{\circ}$C temperature at rotational speed of 75 rpm. Aliquots (10 ml) were withdrawn at different preselected time points and replenished immediately with the same volume of PBS. Finally, the collected resultants were filtered using a membrane filter (0.22 μm, Milipore, USA) and 20 μl of the filtrate was injected into the HPLC (HPLC 820 Metrohm AG, Herisau, Switzerland) using Tris buffer (0.1 M KH_2PO_4 and 0.01 M Tris–HCl), acetonitrile and methanol in the ratio 80:10:10 (v/v) as mobile phase.

2.2c *Characterization techniques*: Powder XRD patterns which were obtained for CaAl-LDH and CaAl-LDH–MTX powders with an X'Pert Pro MPD diffractometer (Panalytical, Almelo, The Netherlands) using Cu$K\alpha$ ($\lambda = 1.5418$ Å) radiation at 40 mA, 40 kV. The step size of 0.03° was used in the scan range 1–40° (2θ). The peak arising from (003) planes of LDH powder was used to calculate the basal spacing in all the samples using Bragg's equation. Crystalline impurities in samples can be readily identified using powder

XRD by simply comparing their characteristic diffraction patterns to a standard reference. By examining the changes in basal spacing of LDH, the possibility of incoming anions towards the successful intercalation or surface adsorption can also be predicted by this technique. FTIR spectra of the as-prepared powders were recorded at room temperature using the KBr (Sigma-Aldrich, $\geq$ 99%) pellet method (sample:KBr = 1:100) on a F Varian 3600 (USA) spectrometer in the 400–4000 cm^{-1} range with an average of 50 scans. Particle morphology and size of CaAl-LDH and CaAl-LDH–MTX samples were examined by TEM using a FEI Tecnai 30 G^2 S-Twin (Netherland) device operated at 300 kV and a Carl Zeiss SMT AG SUPRA 35VP (Germany) field emission scanning electron microscope. The elemental compositions of CaAl-LDH and CaAl-LDH–MTX samples were studied using energy dispersive spectroscopy (EDS) attached to the TEM. Particle sizes of both CaAl-LDH and CaAl-LDH–MTX powders were measured by the DLS technique using a Microtrac Zetatrac, PA (USA) on respective aqueous suspensions. The elemental analyses for CHN of CaAl-LDH–MTX sample were conducted using a model-2400, series II CHN analyser (Perkin-Elmer, USA). Thermogravimetric analyses (TGA) of sample powders were carried out at a heating rate of 10°C min^{-1} in air (thermo-oxidative analysis) from ambient to 1000°C using a NETZSCH STA 409 CD simultaneous thermal analyser. Differential thermal analysis (DTA) provides the information on exothermic and endothermic thermal events that occur in LDH during thermal decomposition. High performance liquid chromatography (HPLC) (Shimadzu LC-20AT, Japan) was used to determine the MTX loading and release from CaAl-LDH–MTX nanovehicle in PBS at pH 7.4.

2.2d *Cell culture*: MG-63 (human osteosarcoma) cells were obtained from ATCC (Rockville, MD, USA, ATCC number CRL-1427). All the cell lines were routinely cultured in Dulbecco's Modified Eagle Medium (DMEM, Invitrogen, Carlsbad, USA) supplemented with 10% heat-inactivated foetal bovine serum, 1 U ml^{-1} penicillin G and 1 mg ml^{-1} streptomycin, at 37°C in a humidified atmosphere of 5% CO_2 in 10 cm (diameter) plastic Petri dishes in a CO_2 incubator (HF90 Heal Force, China). The cells were sub-cultured using trypsin–EDTA when they were 85–90% confluent. All experiments were done with cells when they were within two passages after revival from cryopreservation [22].

2.2e *IC_{50} of MTX*: The IC_{50} (half-maximal inhibitory concentration) of MTX was evaluated at six concentrations in the range 5–100 µg ml^{-1} with a stock solution of MTX (10 mg ml^{-1}) in dimethyl sulphoxide (DMSO, bioreagent grade, Sigma-Aldrich, India). To this, 5×10^3 cell ml^{-1} per well MG-63 cells were plated in a 96-well plate. The cells were then incubated at 37°C in a CO_2 incubator for 24 h to allow sufficient cell adhesion, and the incubation was continued for a total duration of 72 h after addition of MTX to the extent 5, 10, 25, 50, 60, 70, 80, 90 and 100 µg ml^{-1} ($n = 6$). After 72 h, the MTT assay was performed by adding 10 µl 3-(4,5-dimethylthiazole-2-yl)-2,5-phenyltetrazolium bromide) (MTT) reagent at 1 mg ml^{-1} (Sigma Aldrich, USA), in 1:9 ratio (MTT reagent:DMEM medium) to all the wells and this was incubated in dark for a period of 4 h at 37°C. The reaction was stopped by adding 100 µl DMSO to each well of the plate after removal of the MTT and DMEM medium [23]. The absorbance was then measured at 550 nm in an ELISA reader (Bio-Rad, USA), the dose–response curve [24] was generated and the MG-63 cell sensitivity to MTX to inhibit 50% of the cell proliferation was expressed as IC_{50}.

2.2f *Cytotoxicity of CaAl-LDH–MTX nanohybrid*: The assay was performed by plating 5×10^3 cell ml^{-1} (MG-63) per well in a 96-well plate ($n = 6$) and incubated at 37°C for 24 h, as mentioned earlier. MTX drug was then added to each well so that the concentration of MTX was 125 µg ml^{-1} (as per approximately 95.55% cell inhibition from the dose response curve, for determination of IC_{50} of MTX as discussed earlier) per well. The solvent used for MTX was DMSO (analytical grade, Merck, India); 50 µl LDH solution in solvent X, containing 125 µg ml^{-1} of LDH, was then added in each well ($n = 6$); the volume was made up to 200 µl by addition of 150 µl of DMEM medium (without DMSO). In both of these cases (LDH–MTX and LDH), a mixed solvent, solvent X (0.3 M HCL and PBS in the 1:9 volume ratio) was used. The cultured cells (5×10^3 cell ml^{-1}) in DMEM medium was taken as the control. The sets mentioned earlier were made ready individually ($n = 6$) for incubation at 37°C in a humidified atmosphere with 5% CO_2 for a duration 24, 48 and 72 h in a CO_2 incubator (HF90 Heal Force, China), and the cell viability was measured by MTT assay, discussed in detail earlier.

3. Results and discussion

3.1 *XRD analysis*

According to the XRD pattern of CaAl-LDH and its drug intercalated nanohybrid, CaAl-LDH–MTX as shown in figure 1, LDH is well crystallized and exhibits sharp and symmetric peaks at low 2θ angles, but broad and asymmetric peaks at higher 2θ angles, which are the characteristics of clay minerals having layered structure. Because of the layered structure of CaAl-LDH, the crystallites exhibit a preferred orientation; consequently, only 00*l* reflections are seen in the XRD patterns [25,26]. In both the LDH and its intercalates, the 00*l* reflections could be indexed to different interlayer spacings. The gallery height on intercalation of the drug may be obtained by subtracting the brucite layer thickness of 4.8 Å [27,28].

The intercalation of the anionic drug MTX (Scheme 1) into the interlayer space of CaAl-LDH matrix is evidenced by the increase in the interplanar spacing of (003), (006) planes to higher d-values. The basal spacing (d_{003}) of CaAl-LDH is estimated at 8.6 Å ($2\theta = 10.28°$) from the corresponding

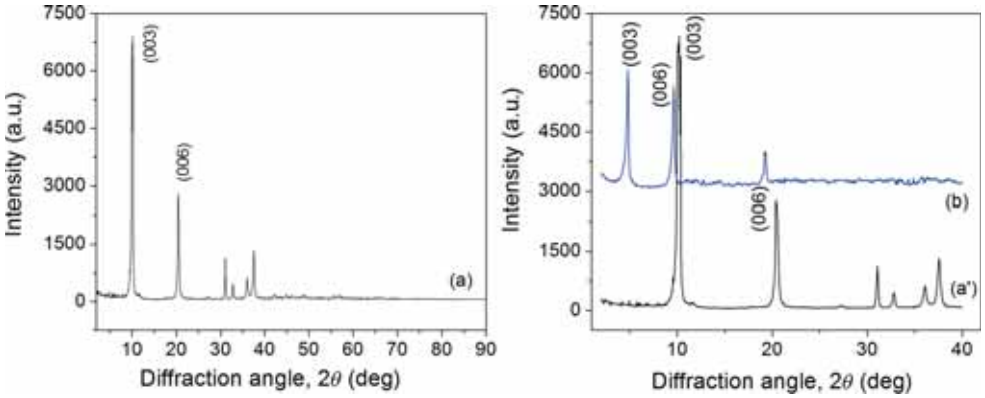

Figure 1. Powder X-ray diffraction patterns of (**a**) pristine CaAl-LDH (2θ = 2–90°) and (**a′**, **b**) pristine CaAl-LDH and CaAl-LDH–MTX (2θ = 2–40°) nanopowders.

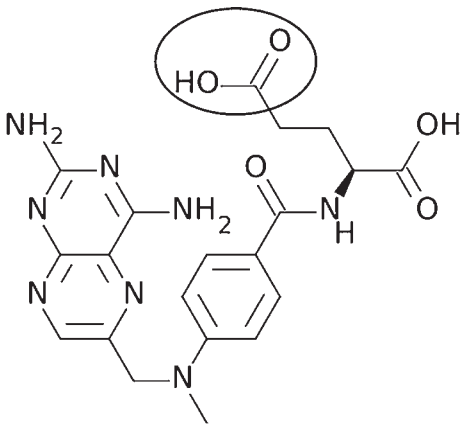

Scheme 1. Molecular structure of methotrexate drug; the anionic counterpart is marked in the circle.

diffraction peak, which is consistent with the LDH structure [29,30]. Arrangement of MTX anions in the interlayer space of LDH occurred in such a manner that the attractive interaction between the cationic octahedral framework and anionic MTX would be the maximum to overcome the repulsive barrier caused by the steric hindrance of large anions and mutual interaction between the positively charged octahedral sheets. The spacing between (003) planes in LDH–MTX is 18.26 Å (2θ = 4.84°) as calculated from the XRD data (figure 1). Considering the sheet thickness of brucite like layer of CaAl-LDH as 4.8 Å, the gallery height of CaAl-LDH–MTX is 13.46 Å [31]. The crystallite sizes were calculated from the second-order reflection only, i.e., (006), using the well-known Scherrer formula:

$$\text{Crystallite size} = k\lambda/(B\cos\theta).$$

Here, B describes the structural broadening, which is the difference in integral profile width between a standard (B_{std}) and the experimental sample (B_{obs}). For this single-profile analysis, NIST 660a was taken as the standard sample, which did not have any size and/or strain broadening, to encompass the effect of instrumental broadening of the diffractometer [9].

From this equation, the crystallite size of LDH and LDH–MTX was found to be 8.7 and 9.26 nm, respectively.

The value of gallery height of CaAl-LDH–MTX is shorter than the longitudinal molecular length of MTX (21.2 Å). Hence, from the gallery heights, it can be calculated that the MTX drug molecule is arranged in a tilted longitudinal monolayer with tilting angle of ∼39.41° to the parallel basal planes of CaAl-LDH–MTX nanohybrid. Such a model allows an enhanced electrostatic interaction between anionic terminal carboxylates of MTX and cationic hydroxide layers. Thus, the drug is intercalated by exchange of nitrate ions of the pristine LDH and is accommodated safely in the interlayer space of LDH by electrostatic interaction.

3.2 *TEM analysis*

Intercalation of MTX into LDH was corroborated from the high-resolution TEM (HRTEM) micrographs of the pristine CaAl-LDH and CaAl-LDH–MTX nanopowders prepared by the co-precipitation method, as shown in figure 2.

HRTEM images showed that the average interlayer spacing in pristine LDH is ∼8.65 Å and it increased to ∼18.32 Å in case of CaAl-LDH–MTX, which is very close to our observations obtained from the XRD data discussed earlier [21].

The TEM image of the LDH crystallites exhibit platelet morphology, which is derived from its hexagonal lattice. The face on image of LDH shows some superimposed as well as distinct platelets, marked by circles in figure 3. There were no significant differences in the morphology of LDH (pristine CaAl-LDH) and its intercalated counterpart (CaAl-LDH–MTX), as per our observation in the face-on image as mentioned earlier; hence, figure 3 exhibits our result corresponding to the pristine CaAl-LDH only [31,32].

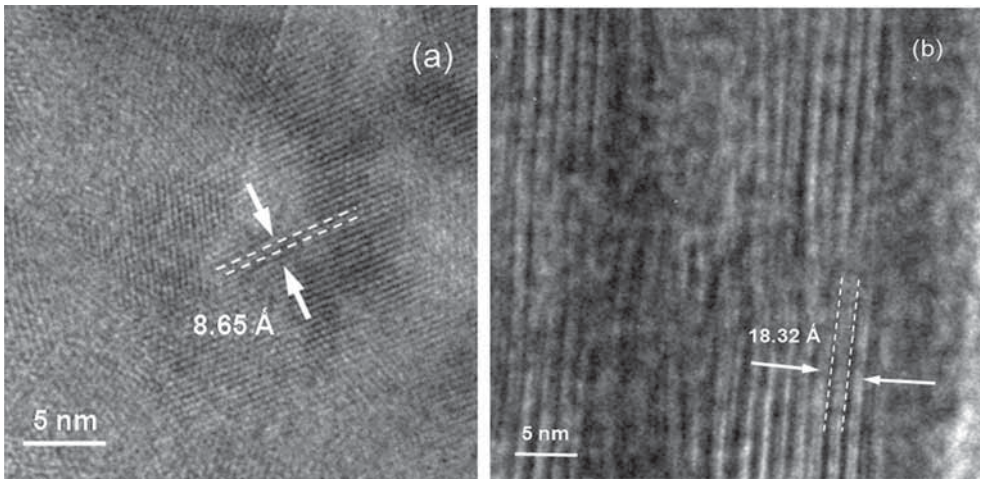

Figure 2. High-resolution TEM images of (**a**) pristine CaAl-LDH and (**b**) CaAl-LDH–MTX nanopowder.

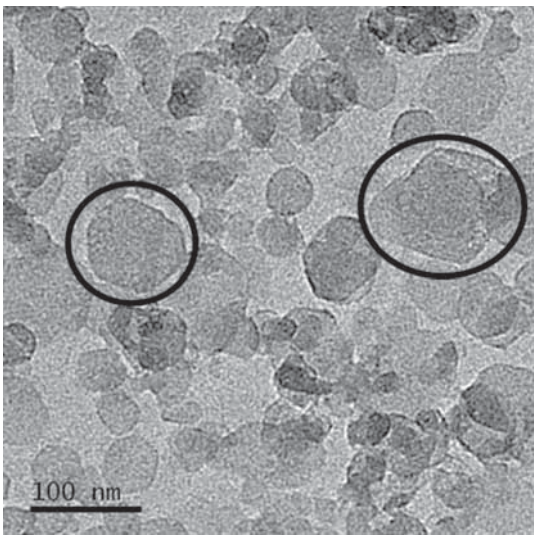

Figure 3. TEM image of pristine CaAl-LDH showing the platelet morphology.

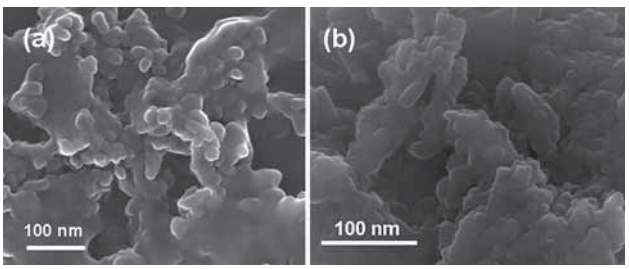

Figure 4. FESEM images of (**a**) pristine CaAl-LDH and (**b**) CaAl-LDH–MTX nanohybrid.

3.3 *FESEM analysis*

FESEM images of pristine LDH and LDH–MTX are shown in figure 4, which shows large clusters of dimension ∼60–80 nm LDH particles having lower aspect ratio as in figure 4a.

After the drug intercalation into the interlayer space of LDH, the aspect ratio of the nanohybrid particle was increased. Elongated nanoparticles with average width of 40 nm and average length of less than 120 nm were observed, as in figure 4b.

3.4 *Thermal analysis*

The TGA of the pristine CaAl-LDH and its drug intercalated counterpart along with the bare drug molecule, as a function of temperature, are shown in figure 5. The TGA trace of CaAl-LDH indicates the mass loss of ∼5.44 and ∼14.10% at a temperature of 90 and 270°C, which is due to the dehydration of physisorbed and structural water molecules, respectively. In LDH–MTX, the total mass loss of ∼15% up to heating of 240°C is due to the removal of surface and structurally bonded water. The weight loss in pristine CaAl-LDH sample increased to ∼38.2% on heating up to 600°C because of the decomposition of interlayer nitrate and carbonate anions. The drug-intercalated samples showed a weight loss of ∼53% on heating up to 600°C because of decarboxylation of MTX and decomposition of nitrate and other charge-balancing anions. On heating up to a temperature of 800°C, ∼41% weight loss in pristine LDH and ∼68% weight loss in LDH–MTX are, respectively, due to the dehydroxylation during spinellization from LDH and oxide-based lattice structure [31,33].

Figure 6 shows DTA curves of CaAl-LDH and CaAl-LDH–MTX prepared by the co-precipitation method, which shows three obvious dehydration peaks corresponding to the mass loss in TG. Dehydration of CaAl-LDH is an endothermic process, which takes place in three main steps, at about 100, 275 and 550°C, as shown in the inset of figure 6. The first

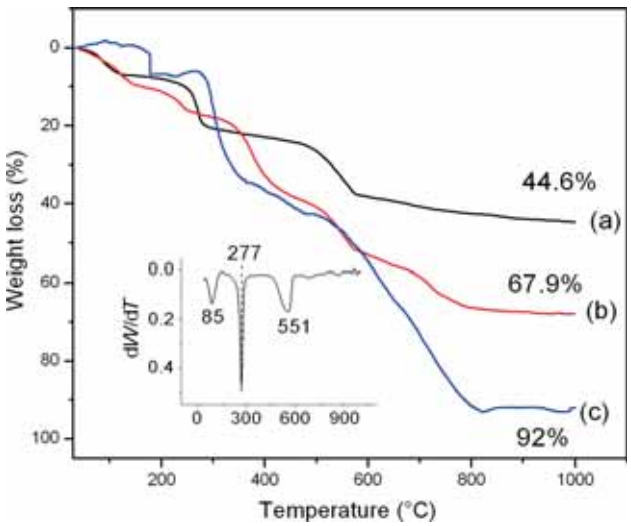

Figure 5. Thermogravimetric analyses of (**a**) pristine CaAl-LDH, (**b**) CaAl-LDH–MTX nanohybrid and (**c**) bare MTX. Derivative of TG plot of pristine CaAl-LDH is given in the inset.

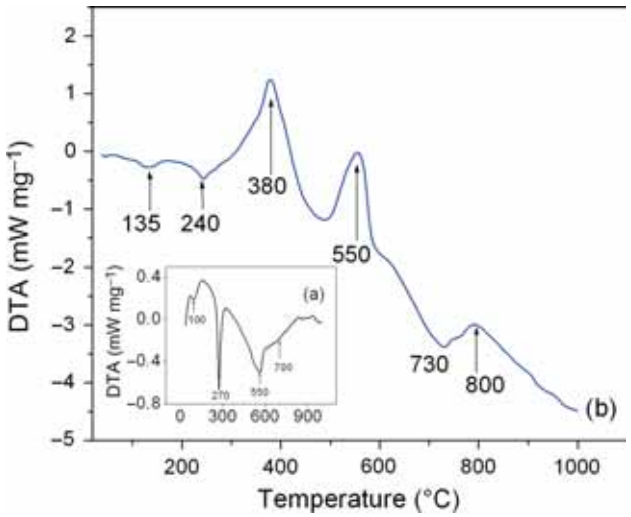

Figure 6. Differential thermal analyses of (**a**) LDH and (**b**) LDH–MTX.

endothermic peak at 100°C is attributed to desorption of physisorbed and interlayer water, which are easily eliminated. Removal of interlamellar water from LDH structure takes place at ∼275°C, followed by dehydroxylation of the lattice and decomposition of interlayer anions at around 550°C. Exothermic peaks at 800 and 900°C indicate the crystallization of $C_{12}A_7$ ($12CaO.7Al_2O_3$) and C_3A ($3CaO \cdot Al_2O_3$) phases [29,32].

LDH–MTX nanohybrid show similar trend in its DTA and TG profiles. The endothermic peaks at 135 and 240°C indicate removal of physisorbed and structural water respectively. Decomposition of MTX is denoted by the exothermic peak at 380°C, whereas exothermic peak at 550°C signifies the decomposition of organic phases into water and gases. The

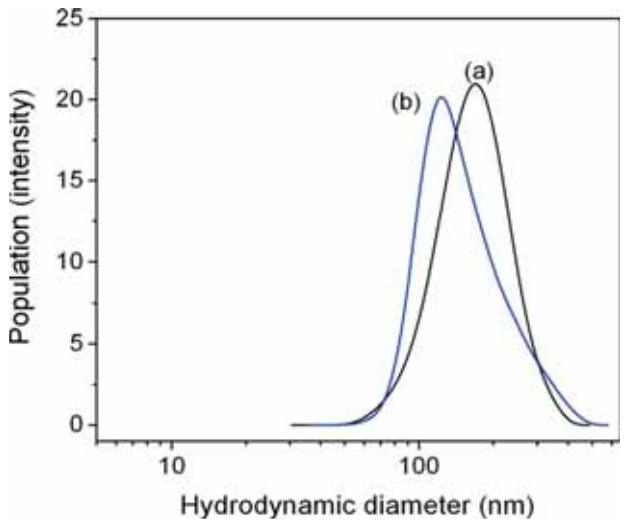

Figure 7. Particle size distribution (intensity) as measured by dynamic light scattering technique of (**a**) pristine CaAl-LDH and (**b**) CaAl-LDH–MTX nanohybrid.

shift in decomposition temperature (∼380°C) of bound MTX molecule in LDH–MTX nanohybrids is somewhat higher as compared to that in unbound MTX (290°C) indicating enhanced thermal stability of MTX in the interlayer position of LDH. Enhanced thermal stability also supports their stable electrostatic interaction with LDH. The exothermic peak at 800°C denotes crystallization into $C_{12}A_7$ ($12CaO \cdot 7Al_2O_3$) and C_3A ($3\ CaO \cdot Al_2O_3$) phases as in the case of CaAl-LDH before [34].

Based on TGA, the loading of MTX in CaAl-LDH by the co-precipitation method is estimated as 49.2 wt%. This is in good agreement with the MTX loading estimated from the CHN analysis.

3.5 *Particle size analysis*

Particle size is one of the most critical factors influencing cell adhesion, uptake behaviours and intracellular processing of nanoparticles and it is known from the literature that the particle size of LDHs should fall in the range of 100–200 nm for higher uptake and longer retention in the cells.

The hydrodynamic sizes of pristine and MTX-intercalated CaAl-LDH by co-precipitation methods in aqueous slurry were measured by light scattering and are given in figure 7. The average hydrodynamic diameter (Z_{av}) of pristine LDH particles in aqueous suspension is ∼168 nm with the majority of the particles in LDH below 200 nm. The size distribution is unimodal and the calculated polydispersity index (PDI) from the size data is 0.233. The hydrodynamic diameters slightly decreased on MTX intercalation by the co-precipitation method. After intercalation of MTX by the co-precipitation method the hydrodynamic diameters of LDH decreased to ∼122 nm (PDI 0.316) as was also observed from FESEM (figure 4).

In the DLS technique, almost all the particles in CaAl-LDH and its intercalated counterpart have particle sizes below 200 nm, suggesting that most of these nanocarriers can reach the target cells during the drug delivery [30].

3.6 *Drug release study*

The purpose of the drug release study is to investigate the effective delivery of the encapsulated drug, MTX here, from the LDH nanovehicle in a controlled manner that works eventually for enhancing the drug efficacy. This also provides information about the kinetics of release of the drug by choosing the best-fitting model of the same. The release behaviour as change in concentration of MTX in PBS medium from LDH–MTX nanohybrid at physiological pH (7.4) is shown in figure 8 to evaluate its potential as a drug carrier. The initial faster release of ∼20% of MTX from LDH–MTX in 2 h incubation in PBS solution was due to desorption of loosely bound MTX from the surface of LDH–MTX nanohybrid. This was followed by a constant rate of release of another ∼22% MTX from LDH–MTX in a period of 2–6 h due to detachment of strained MTX molecule bound to LDH lattice. Later, nearly ∼18% release of MTX from LDH–MTX within a period of 6–10 h of incubation was due to de-intercalation of anionic drug from the interlayer space because of electrostatic interaction between anionic species in PBS, including carbonate and bicarbonate coming from air and cationic octahedral framework. Further release of ∼13% of MTX over a period of 10–24 h incubation of CaAl-LDH–MTX nanohybrid prepared by co-precipitation method was due to a combination of de-intercalation of MTX and crystal dissolution of LDH–MTX nanohybrid. A slow but sustained release of remaining ∼27% of MTX from LDH–MTX (co-precipitation) up to a period of 120 h was primarily because of detachment of tightly bound MTX molecule in the course of gradual dissolution of LDH–MTX nanohybrid at pH 7.4 [35].

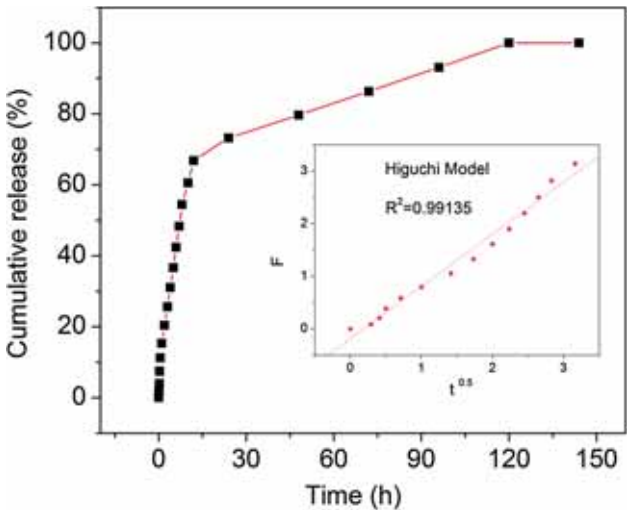

Figure 8. Cumulative release rate of MTX from CaAl-LDH–MTX nanohybrid as a function of time and fit of cumulative released fraction of MTX from CaAl-LDH–MTX nanohybrid with respect to incubation time (t) following the Higuchi model, shown in the inset.

The *in vitro* release profile of MTX from CaAl-LDH–MTX nanohybrid was analysed by various kinetic models. The kinetic models used were zero-order, first-order, Higuchi and Korsmeyer–Peppas equations (figure 9). The cumulative release profile of MTX from MTX-loaded LDH nanoparticles and its best-fit model (inset) are shown in figure 8. The release constants were calculated from the slope of the respective plots and have been listed in table 1. It is known that for planar geometry, the value of $n = 0.37$ indicates a Fickian diffusion mechanism ($0.37 < n < 0.45$). The release profile of the drug from the nanoparticles showed the best fitting to the Higuchi model as per the correlation coefficient value ($R^2 = 0.9913$) having kinetic exponent of $n = 0.37$, which confirms the release of the drug following Fickian diffusion mechanism from the nanoparticle matrix system, at pH 7.4.

As the drug release is due to the exchange of drug anions with the anions of the PBS dissolution medium, once exchanged, the drug anions diffuse through the LDH particle and then through the diffusion layer. Thus the drug release

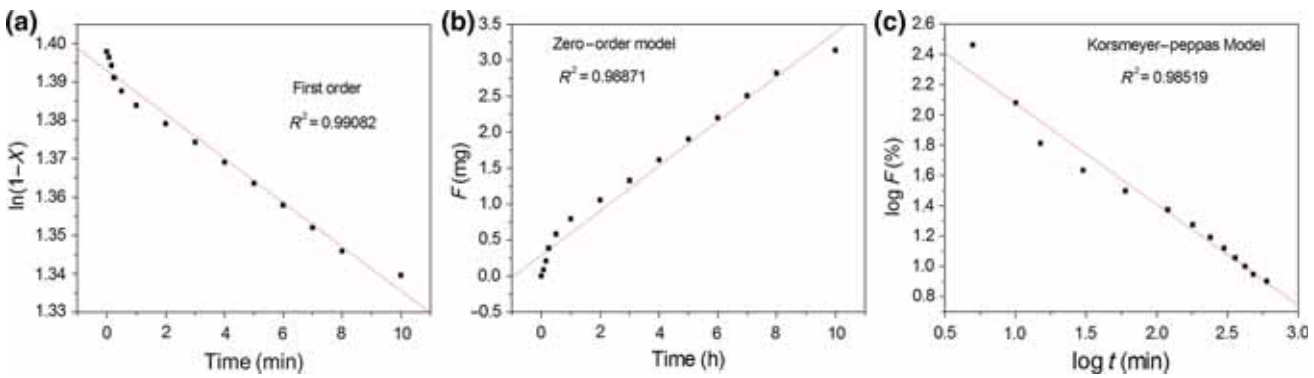

Figure 9. MTX release profile from CaAl-LDH–MTX matrix as a function of time and its plot following (**a**) first–order, (**b**) zero-order and (**c**) K–P release kinetics model for the release of MTX from the nanohybrid.

Table 1. Drug release kinetic parameter for CaAl-LDH–MTX.

Code	First order	Higuchi	Zero order	K–P model	
CaAl-LDH–MTX	$R^2 = 0.9908$	$R^2 = 0.9913$	$R^2 = 0.9887$	$R^2 = 0.9852$	$n = 0.37$

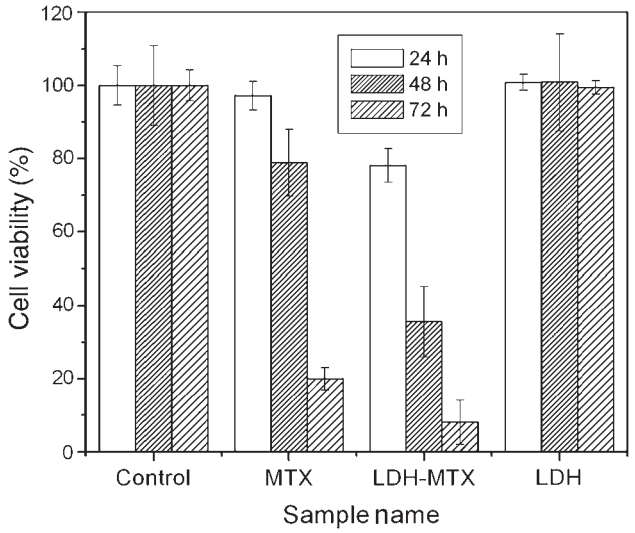

Figure 10. The cytotoxicity assay of CaAl-LDH–MTX using MG-63 cell line up to 72 h.

could be controlled by the diffusion through the LDH particle, or by the diffusion through the layer surrounding the particle. In such a process, the rate of exchange of drug ions between the LDH and the PBS dissolution medium would be ultimately determined by the slower of these two processes, considering the variation in charge and type of anions (MTX and PO_4^{3-}) [36].

3.7 *In vitro cytotoxicity assay*

For the viability study, cells were exposed to 250 μg ml^{-1} concentrations of CaAl-LDH–MTX nanohybrid.

Figure 10 shows the efficacy of CaAl-LDH–MTX in inhibiting the growth of human osteosarcoma cells (MG-63) at different incubation times. Interestingly, bare MTX drug and its LDH-intercalated nanohybrid play an important role in inhibiting the cancer cell growth, whereas the ceramic nanocarrier shows no significant effect. Cell viability was measured using the MTT assay, which is based on the reduction of yellow tetrazolium MTT salt by metabolically active cells, leading to the formation of purple formazan crystals. On comparing the IC_{50}, the concentration that inhibits 50% of the cellular growth, LDH–MTX shows lower IC_{50} compared with the value of free drug. This finding indicates that the intercalated compound has higher inhibitory effects towards the MG-63 cells compared with that of free drug. It was found that after 24 h of administration the effect of the LDH–MTX nanohybrid starts, and it exhibits ∼22% inhibition of cell growth in comparison with the bare drug MTX (∼3%). After 48 h, the efficacy of this nanohybrid is enhanced remarkably to three times (from ∼22 to 65%), whereas the action of the bare drug is much slower (∼9 to 22%) only. A much higher efficacy of LDH–MTX nanohybrid, compared with its bare drug counterpart monitored is distinctly noticeable for a period of 72 h. The LDH–MTX nanohybrid exhibits cell inhibition to the extent of ∼92%, whereas in case of the bare drug, it is ∼80%. This confirms the higher efficacy of the nanohybrid in comparison with the bare drug, on account of the enhanced stability and increased plasma half-life of MTX in an encapsulated status.

Hence, the potential of the LDH nanoparticles as an excellent drug delivery vehicle is confirmed, for subsequent use of a gamut of drugs of similar category and application area.

Considering the sustained release behaviour of CaAl-LDH–MTX, we would attribute the enhanced antiproliferative effects observed in LDH–MTX to the strong interactions occurring between LDH and MTX; the host ceramic carrier would facilitate the cell uptake and further protect the guest MTX molecule from degradation so that the anions are slowly released and 'kill' the MG-63 cells.

4. Conclusions

CaAl-LDH nanocarrier was synthesized by a simple, one-pot co-precipitation method at room temperature, with simultaneous *in-situ* incorporation of chemotherapeutic drug MTX. Intercalation of MTX in the interlayer space of CaAl-LDH was confirmed from XRD and HRTEM analyses followed by FTIR spectroscopy, which clearly revealed the exchange of the nitrate anion of the pristine CaAl-LDH by the MTX drug molecule. The particle sizes of pristine CaAl-LDH and its drug intercalated counterpart were found to be in the range of 100–170 nm, obtained by the DLS technique. The thermal analysis revealed an increase in decomposition temperature of MTX bound to CaAl-LDH nanohybrid, indicating a strong interaction between the anionic MTX and cationic brucite-like layers. Cumulative release of MTX from CaAl-LDH–MTX in phosphate buffer solution (pH 7.4) showed a non-linear pattern of release of MTX with incubation time that was governed by diffusion mechanism at physiological pH of 7.4. The antiproliferative action towards MG-63 cells was enhanced due to the synergistic effect of LDH–MTX, compared with MTX. These findings should

serve as strong foundations in further development of the biocompatible LDH-based drug carriers for drug delivery applications.

Acknowledgements

We are grateful to the Director, Central Glass and Ceramic Research Institute, Kolkata, India, for giving permission and facilities to carry out this work. Thanks are due to all the supporting staff for various characterization works. This work was supported financially by the Council of Scientific and Industrial Research, New Delhi, via project number NWP 0035, of 11th 5-year plan network program.

References

[1] Cho K J, Wang X, Nie S M, Chen Z and Shin D M 2008 *Clin. Cancer Res.* **14** 1310
[2] Faraji A H and Wipf P 2009 *Bioorg. Med. Chem.* **17** 2950
[3] Li F and Duan X 2006 In: *Structure and bonding* (Berlin: Springer) vol 119 p 193
[4] Zhang F Z, Xiang X, Li F and Duan X 2008 *Catal. Surv. Asia* **12** 253
[5] Aguzzi C, Cerezo P, Viseras C and Caramella C 2007 *Appl. Clay Sci.* **36** 22
[6] Palmer S J, Frost R L and Nguyen T 2009 *Coord. Chem. Rev.* **253** 250
[7] Prasanna S V, Kamath P V and Shivakumara C 2007 *Mater. Res. Bull.* **42** 1028
[8] Chakraborty M, Dasgupta S, Sengupta S, Chakraborty J, Ghosh S, Ghosh J *et al* 2012 *Ceram. Int.* **38** 941
[9] Chakraborty M, Dasgupta S, Soundrapandian C, Chakraborty J, Ghosh S, Mitra M K *et al* 2011 *J. Solid State Chem.* **184** 2439
[10] Newman S P and Jones W 1998 *New J. Chem.* **22** 105
[11] Olfs H W, Torres-Dorante L O, Eckelt R and Kosslick H 2009 *Appl. Clay Sci.* **43** 459
[12] Xiang X, Hima H I, Wang H and Li F 2008 *Chem. Mater.* **20** 1173
[13] Cavani F, Trifro F and Vaccari A 1991 *Catal. Today* **11** 173
[14] Li Y, Liu D, Ai H H, Chang Q, Liu D D, Xia Y *et al* 2010 *Nanotechnology* **21** 105101
[15] Li B X, He J, Evans D G and Duan X 2004 *Appl. Clay Sci.* **27** 199
[16] Del Arco M, Cebadera E, Gutierrez S, Martin C, Montero M J, Rives V *et al* 2004 *J. Pharm. Sci.* **93** 1649
[17] Choy J H, Jung J S, Oh J M, Park M, Jeong J, Kang Y K *et al* 2004 *Biomaterials* **25** 3059
[18] Nakayama H, Takeshita K and Tsuhako M 2003 *J. Pharm. Sci.* **92** 2419
[19] Lee J H and Jung D Y 2012 *Chem. Commun.* **48** 5641
[20] Khan A I, Lei L X, Norquist A J and O'Hare D 2001 *Chem. Commun.* **22** 2342
[21] Plank J, Dai Z and Andres P R 2006 *Mater. Lett.* **60** 3614
[22] Mandal S, Chatterjee N, Das S, Saha K D and Chaudhuri K 2007 *RSC Adv.* **4** 20077
[23] Liu W M and Dalgleish A G 2009 *Chemother. Pharmacol.* **64** 861
[24] Walters D K, Muff R, Langsam B, Born W and Fuchs B 2008 *Invest. New Drugs* **26** 289
[25] Gago S, Costa T, de Melo J S, Goncalves I S and Pillinger M 2008 *J. Mater. Chem.* **18** 894
[26] Roman M S S, Holgado M J, Jaubertie C and Rives V 2008 *Solid State Sci.* **10** 1333
[27] Radha A V, Kamath P V and Shivakumara C 2005 *Solid State Sci.* **7** 1180
[28] Xu Y, Dai Y, Zhou J, Xu Z P, Qian G and Lu G Q M 2010 *J. Mater. Chem.* **20** 4684
[29] Plank J, Keller H, Andres P R and Dai Z 2006 *Inorg. Chim. Acta* **359** 4901
[30] Giraudeau C, De Lacaillerie J B D, Souguir Z, Nonat A and Flatt R J 2009 *J. Am. Ceram. Soc.* **92** 2471
[31] Shafiei S S, Solati-Hashjin M, Rahim-Zadeh H and Samadikuchaksaraei A 2009 *Adv. Appl. Ceram.* **112** 59
[32] Matusinovic Z, Rogosic M and Sipusic J 2009 *Polym. Degrad. Stabil.* **94** 95
[33] Puttaswamy N S and Kamath P V 1997 *J. Mater. Chem.* **7** 1941
[34] Manzi-Nshuti C, Chen D, Su S and Wilkie C A 2009 *Thermochim. Acta* **495** 63
[35] Li F, Jin L, Han J, Wei M and Li C 2009 *Ind. Eng. Chem. Res.* **48** 5590
[36] Dave B S, Amin A F and Patel M M 2004 *AAPS Pharm. Sci. Tech.* **5** 77